Technical Challenges & Opportunities of PET/MR: An Overview

Harald H. Quick, PhD

Institute of Medical Physics
University of Erlangen, Erlangen, Germany
Harald.Quick@imp.uni-erlangen.de

Highlights

- Following PET/CT, PET/MR is the newest diagnostic whole-body hybrid imaging modality.
- Simultaneous PET and MR data acquisition requires novel technical solutions and offers new diagnostic opportunities.
- Attenuation correction (AC) and motion correction (MC) of PET data are current hot topics in PET/MR hybrid imaging research.
- The added diagnostic value of PET/MR in whole-body imaging is currently under investigation.

INTRODUCTION

Integrated whole-body PET/MR hybrid imaging combines excellent soft tissue contrast and various functional imaging parameters provided by MR with high sensitivity and quantification of radiotracer metabolism provided by PET.

Integrated PET/MR demands for new technologies and innovative solutions, currently subject to interdisciplinary research. Attenuation correction of human soft tissues and of hardware components has to be MR-based to maintain quantification of PET imaging since CT attenuation information is missing. This brings up the question of how to provide bone information with MR imaging. The limited field-of-view in MR imaging leads to truncations in body imaging and MR-based attenuation correction. Another research field is the implementation of motion correction technologies to correct for breathing and cardiac motion in view of the relatively long PET data acquisition times. While these technical challenges are currently under investigation, integrated PET/MR offers new diagnostic opportunities in oncology, neurology, pediatric oncology and cardiovascular disease (1).

TECHNICAL CONSIDERATIONS

Integrated PET/MR System Technology

To achieve a full integration of an MR and PET imaging modality in one whole-body system, numerous physical and technical preconditions and challenges had to be overcome (Fig. 1). The potential physical interactions of both modalities in both directions – PET on MRI and MRI on PET – are manifold. Full integration of a PET system into an MRI environment required technical solutions such that PET hardware and PET signals are not disturbed by any of the electromagnetic fields of MR. Equally, for full and unlimited MRI system performance, PET must not disturb any of these electromagnetic MR fields and signals (2).

One current example of an integrated whole-body PET/MR system is the Biograph mMR (Siemens Healthcare Sector, Erlangen, Germany) (Fig. 1) (1,2). This hybrid system comprises a 3.0 Tesla whole-body MR system with a length of 199 cm (magnet length 163 cm) that hosts a fully integrated PET detector in its magnet isocenter providing a 60 cm diameter patient bore. Maximum gradient strength is 45 mT/m in all three axes and maximum slew rate is 200 mT/m/ms. The PET unit comprises a total of 56 LSO-APD detector blocks, each consisting of 64 crystal elements with a block area of 32 x 32 mm^2. The blocks are aligned circumferentially to form one PET detector block ring (Fig. 1). Eight detector block rings form the full PET detector unit, spanning a field of view of 25.8 cm in z-direction (2).

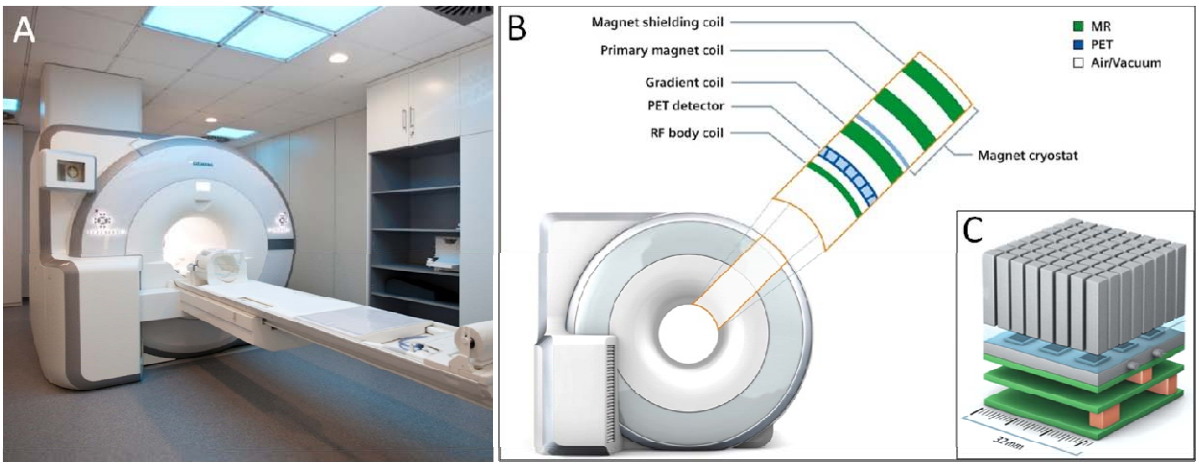

Figure 1: **(A)** Integrated PET/MR System (Biograph mMR, Siemens AG, Healthcare Sector) installed at the Institute of Medical Physics, University of Erlangen, Germany. **(B)** Schematic drawing showing the integration of the PET detectors in the MR hardware structure. From the inside to the outside: RF body coil, PET detector, gradient coil assembly, primary magnet coil, and magnet shielding coil. **(C)** PET detector assembly where 64 Lutetium Oxyorthosilicate (LSO) crystals form one detector block.

Attenuation Correction (AC)

PET data needs to be attenuation corrected in the reconstruction process in order to provide a valid quantification of tracer activity distribution in the human body. Scanner hardware components (e.g. table top, RF coils, etc.) as well as patient tissues within the FOV of the PET detector during data acquisition attenuate the number of true annihilation events and consequently lead to false results without AC. Depending on the relative position of an active lesion in the patient's body, the associated gamma quanta experience different attenuation on their way through different body tissues to the PET detector. Non-AC PET data generally shows underestimation of the tracer activity deep in the patient's body. Since the PET/MR hybrid system cannot measure linear attenuation directly as in PET/CT hybrid imaging, AC here needs to be performed differently.

Hardware Component AC

Radiofrequency surface receiver coils are a technical precondition for high resolution MR imaging and are well established in clinical MRI. In integrated PET/MR imaging, the RF surface coils cover the patient's body during simultaneous MR and PET data acquisition. Thus, all RF surface coils have to be optimized for PET-transparency, i.e. such coils should attenuate gamma quanta only minimally (3-6).

The PET signal attenuation of rigid and stationary equipment such as the RF spine array and the RF head/neck coil can be compensated for by straightforward AC methods.

After scanning this equipment by using CT, a 3-dimensional (3D) map of attenuation values can be generated. This data can then be converted into a 3D representation of the 511 keV attenuation values, the so-called “µ-map”. By linking the RF spine – or RF head coils position to the patient’s table position, the corresponding AC µ-map for each table position is automatically selected by the system for PET image reconstruction. Another recent example of hardware component AC is the integration of a 4-channel RF breast coil into the concept of PET/MR breast imaging (Fig. 2) (7). The RF breast coil in that study has been selected regarding its PET transparency and is used in conjunction with CT-based 3D attenuation maps (Fig. 2C,D) that are completed with MR-based patient soft tissue AC for overall AC of PET data (Fig. 2E).

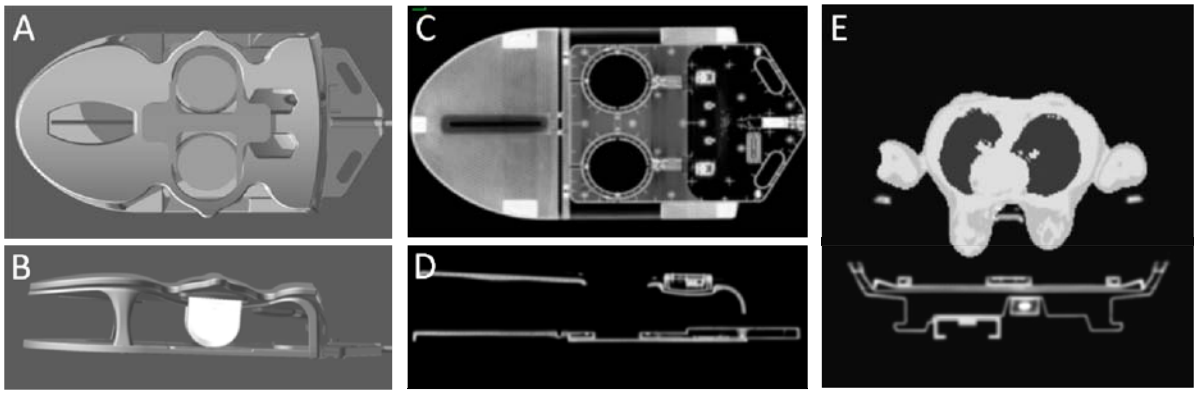

Figure 2: Computer rendering of a 4-channel radiofrequency (RF) breast coil with breast phantoms for integrated PET/MR breast imaging in coronal **(A)** and sagittal **(B)** orientation. Corresponding CT-based hardware attenuation map of the RF breast coil in coronal **(C)** and sagittal **(D)** orientation. Image **(E)** shows the combined CT-based hardware (patient table and RF breast coil) and MR-based soft tissue attenuation map of a female patient in transversal orientation.

Human Tissue AC

Attenuation correction of human soft tissue is necessary to correct for the individual patient anatomy. Since no linear attenuation coefficient-based CT information is available in integrated PET/MR hybrid imaging, tissue specific AC has to be based on MR information which is based on proton density and relaxation properties (e.g. T1 and T2 relaxation times), rather than on the attenuation of X-rays in tissue. Both air and solid bone lack signal in MRI, thus these fundamentally different tissue classes are difficult to separate. In the current implementation of integrated PET/MR systems, tissue attenuation and scatter correction is performed using a 3D Dixon-VIBE technique, providing two sets of images where water and fat are “in phase” and “out-of phase” (Fig. 3) (8). This allows reconstruction of fat-only, water-only and fat-water images and results in tissue segmentation of air, fat, muscle, and lungs in the reconstructed and displayed µ-maps (Fig. 3) (8). Cortical bone is currently not being accounted for in the Dixon-based MR-AC approach. Bone is here classified as soft tissue and thus the exact magnitude of PET signal attenuation of bone might be underestimated (9).

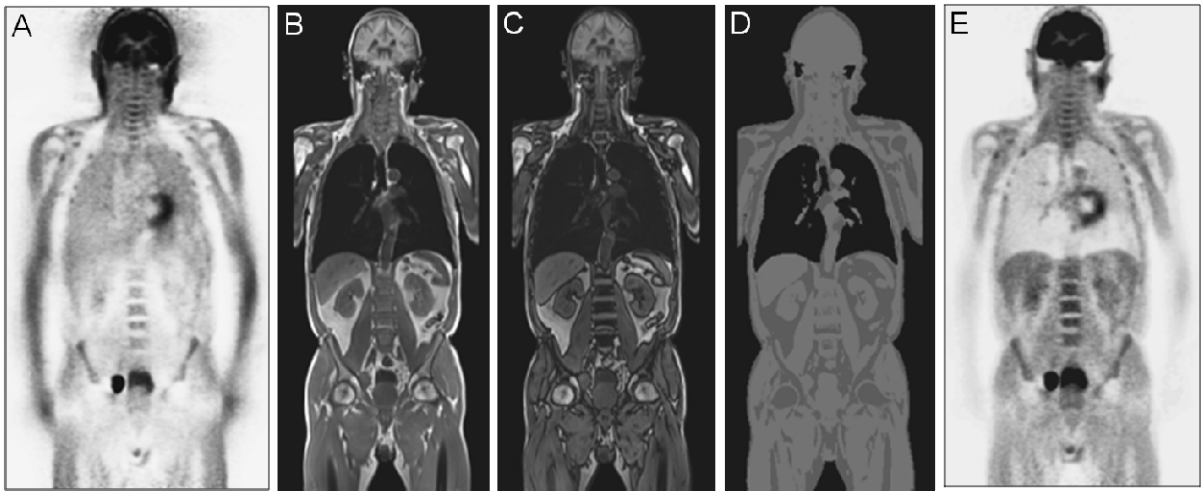

Figure 3: Soft-tissue attenuation correction (AC) based on MR imaging. **(A)** Uncorrected whole-body PET scan showing relative activity enhancement in the lungs and along the outer contours of the patient. (**B,C**) Dixon-VIBE MR sequence providing separate water/fat "in-phase" and "opposed phase" images that serve as basis for soft-tissue segmentation. **(D)** Segmented soft tissue groups (air, fat, muscle, lungs) that can be assigned to a PET attenuation map. **(E)** Resulting attenuation corrected whole-body PET scan of the initial data set **(A)**.

Bone in AC

Since bone and air both do not provide signal in conventional MRI sequences, bone is currently not considered in MR-based AC. In current Dixon based methods, bone is assigned the LAC of soft tissues during tissue segmentation (8). This leads to a systematic underestimation of the attenuating effects of bone during MR-based AC (9).

Current methods for MR-based AC include ultrashort echo time (UTE) sequences able to also display tissues with very short T2* (e.g. bone) (10,11). This is to render information about trabecular and cortical bone that then will be assigned LAC of bone during image segmentation (Fig. 4). Further refinements of the method have been pursued to include pattern recognition knowledge (support vector regression, SVR) (12). This method recently succeeded in assigning continuous LAC instead of only 3-4 discrete LAC for limited number of tissue classes (Fig. 4) (12). While UTE-based protocols and combinations of UTE with Dixon sequences have been validated in the head region in numerous initial studies (10,11), the application to other body regions is still at the beginning (12) (Fig. 4C).

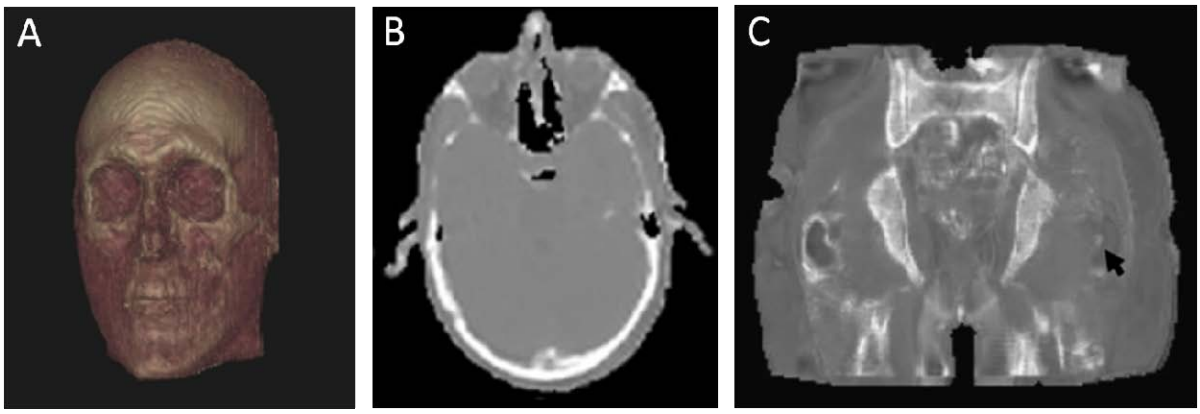

Figure 4: Adding bone to MR-based attenuation correction (AC) with UTE sequences. Three-dimensional rendering of MR-based bone information **(A)** of a patient. MR-based "pseudo-CT attenuation map **(B)** for attenuation correction of PET data that was acquired using a Dixon-VIBE and UTE sequence and pattern recognition information. Coronal view **(C)** of MR-predicted "pseudo-CT" data acquired in the pelvis of a volunteer using the Dixon-VIBE and UTE acquisition model.

Motion Correction (MC)

Integrated PET/MR systems provide the inherent advantage of simultaneous PET and MR data acquisition. In view of motion correction (MC) this is an inherent advantage over PET/CT that is currently being further explored (13). While in PET/CT the CT data is static and for dose considerations is acquired only once at the beginning at a typical hybrid examination, the MR data in PET/MR is acquired simultaneously to PET data acquisition and this applies to data acquisition in each bed position. This inherently leads to less deviation and less gross motion between both imaging modalities when compared to PET/CT imaging. Furthermore, real-time MRI data and 4D MR data of breathing motion can be used to retrospectively motion correct PET data to provide improved fusion of PET and MR data sets (14,15). This may potentially lead to improved lesion visibility in the lungs, upper abdomen, and liver and may also result in better lesion quantification since lesions are better depicted and less smeared over a larger volume which otherwise leads to reduced standardized uptake values (SUV) of lesions subject to motion (14).

CLINICAL APPLICATIONS

Hybrid imaging with PET/MR is generally characterized with providing excellent soft tissue contrast paired with the high inherent sensitivity of PET regarding the detection of metabolism of specific radiotracers. At the same time PET/MR provides these diagnostic features while reducing overall radiation dose when compared to PET/CT examinations. It is thus to be expected that PET/MR will outperform PET/CT in diagnostic value in selected applications where MR is superior to CT. Beyond the scope of initial clinical PET/CT vs. PET/MR comparison studies (16-19) integrated PET/MR hybrid imaging is now under evaluation to define its diagnostic value in various clinical applications in oncology, neurology, pediatric imaging, cardiovascular disease, and therapy planning and response monitoring.

Oncologic Disease

Among the first studies evaluating the diagnostic potential of PET/MR are intraindividual PET/CT vs. PET/MR comparison studies on oncologic patients encompassing a broad spectrum of tumor entities (16-19) (Fig. 5). PET/MR imaging in this oncologic patient population is applied to cover single organ region to whole-body tumor staging and metastasis screening. Lesion detection rates in these studies showed high correlation values (>90%) for detection of congruent lesions in PET/CT as well as PET/MR (16-18). Quantification of lesion activity with PET/CT compared to PET/MR, however, indicated somewhat lower SUV for PET/MR compared to identical lesions measured with PET/CT. A potential explanation for these differences is the fact that in all these comparison studies PET/CT has been performed first, then followed by PET/MR. Starting time of the PET/MR exam thus was delayed by several hours when compared to PET/CT (16-19). Consequently, the advanced tracer metabolism and biodistribution over time might have had an influence on lesion quantification. Another potential source of error is the MR-based attenuation correction with the above listed shortcomings (segmentation into discrete tissue classes, missing bone information, FOV truncation, etc). These aspects should not be overrated since first clinical studies overall show very good, robust and reproducible results, however, deserve further investigation in carefully designed studies systematically separating physiological effects of tracer dynamics from technical and methodological effects.

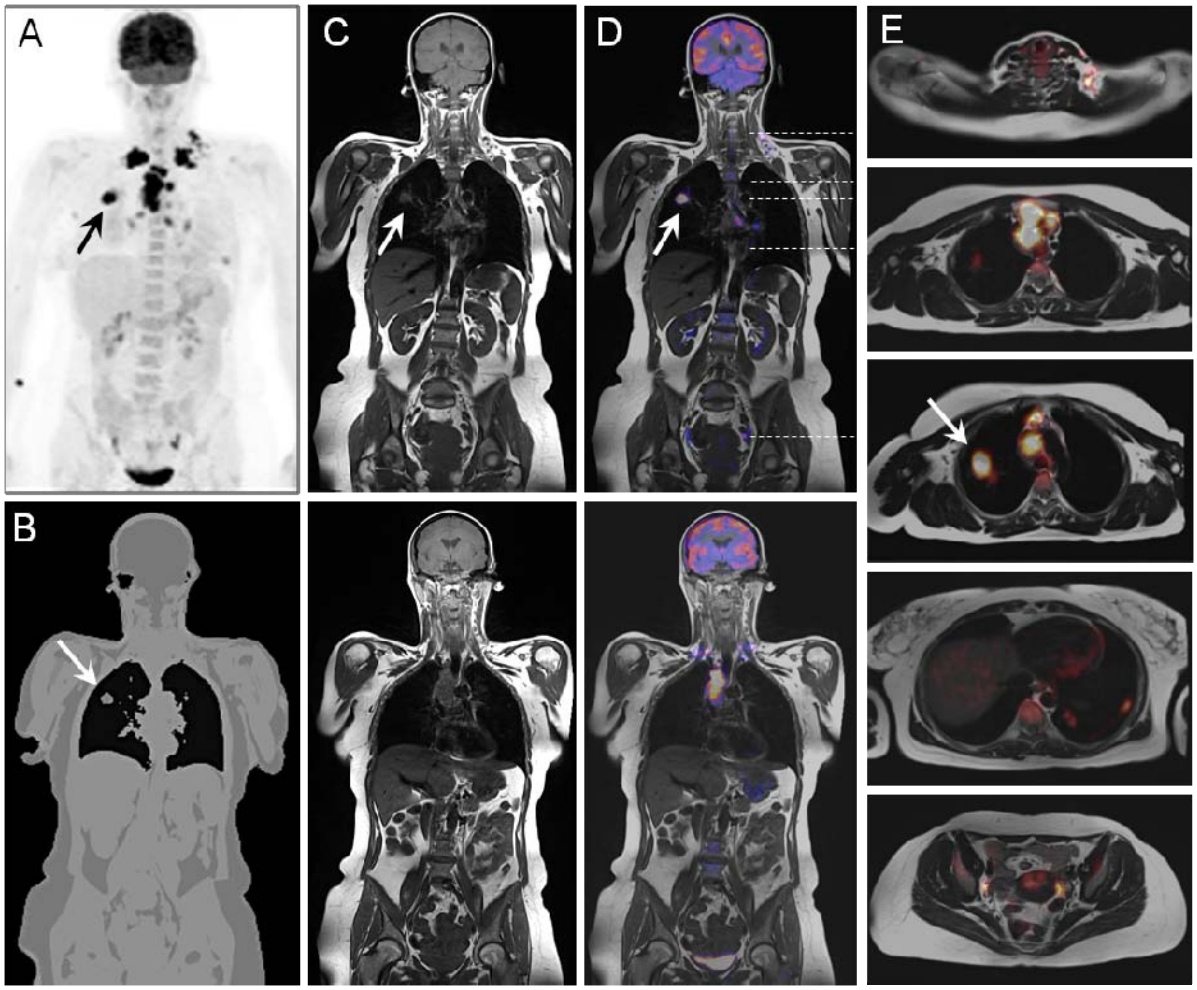

Figure 5: 44 year old female with bronchial carcinoma (NSCLC, stage IV). **(A)** PET data (236 MBq F18 FDG), **(B)** MR-based attenuation map for AC (3D Dixon-VIBE) of human soft-tissue. **(C)** T1-weighted coronal views of two planes. **(D)** PET/MR data fusion of the two planes shown in **(C)**. **(E)** Axial PET/MR views at different body levels show FDG-positive lesions in the left supraclavicular groove, ipsi- and contralateral mediastinum, and contralateral lung. There are additional FDG-positive lymph nodes in bilateral iliac lymph nodes. Arrows point to an identical lesion in different views.

Neurologic Disease

In diagnosis of neurologic disease integrated PET/MR unveils its full morphologic and functional potential. The diagnostic power of MR in neuro imaging here is multiplied with the capabilities of PET using various specific tracers. Since PET and MR data are acquired simultaneously at one bed position only, the overall acquisition time can be invested in multiple contrast weightings, spectroscopic information (Bisdas 20), and also in adding dynamic information in PET and/or MR. Contrast agent dynamics (in MR) as well as tracer metabolism (in PET) can be monitored over time (21). First results applying amyloid specific PET tracers in PET/MR have shown to support the diagnosis of Alzheimer's disease (22).

Pediatric Oncology

In pediatric oncology, MR can provide valuable diagnostic information complementary to PET or PET/CT (23) (Fig. 6). Moreover, considering dose aspects, PET/MR can be seen as a valuable alternative to PET/CT imaging for longitudinal follow-up studies monitoring the therapeutic response to chemotherapy. Although data is still sparse, first studies have demonstrated impressive diagnostic results (23). Potential dose savings of up to 80% have been postulated when using PET/MR instead of PET/CT in pediatric oncologic imaging (23).

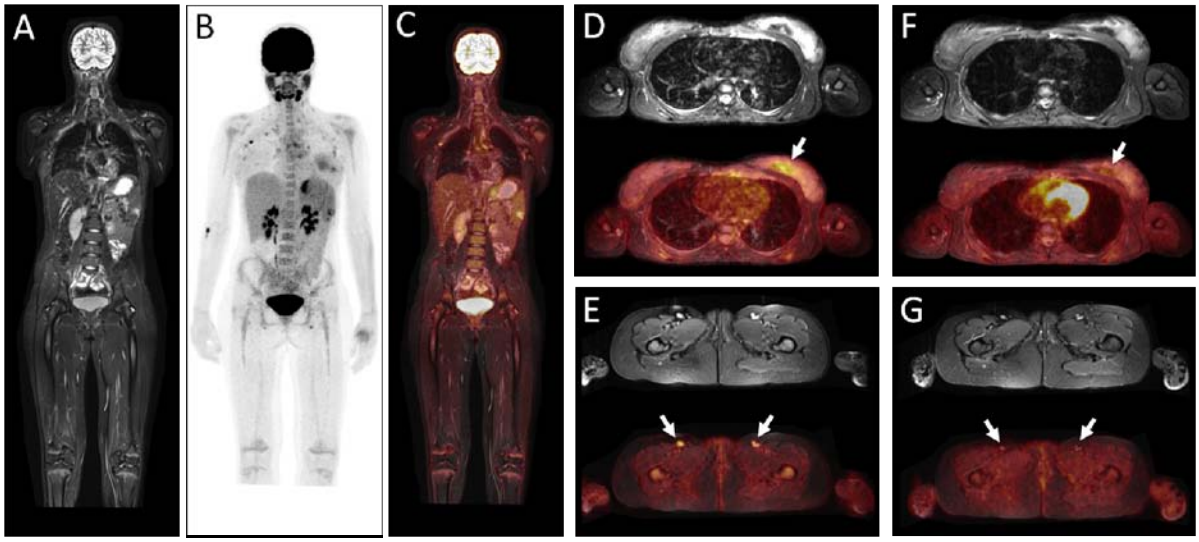

Figure 6: 14 year old female patient that was diagnosed with acute myeloid leukemia (AML). Primary staging with integrated PET/MR **(A-C)** revealed renal, pancreatic, mammary, splenic, and lymph node involvement. Chemotherapy was thus commenced. PET/MR imaging at 1 months follow-up after start of chemotherapy **(D,E)** revealed residual tumor in left mammary formation (SUV_{max} = 3.6) (arrow in **D**) and residual tumor in inguinal lymph nodes (SUV_{max} = 3.1) (arrows in **E**). PET/MR imaging at 2 months follow-up after start of chemotherapy **(F,G)** shows a complete response to chemotherapy and no sign of increased tracer activity in the same regions (arrows in **F,G**). Courtesy of Dept. of Nucl. Medicine (Director: Prof. Dr. O. Sabri), University of Leipzig, Germany.

Challenge	Correction method	Reference #
▪ Attenuation correction (AC) of hardware components	▪ CT-based and energy converted templates of hardware components	3-6
▪ Attenuation correction (AC) of human tissues	▪ MR-based tissue segmentation into tissue classes with Dixon-sequences	8
▪ Adding bone information to MR-based attenuation correction	▪ MR-based bone segmentation with ultrashort echo time sequences (UTE) ▪ Training data using pattern recognition methods (SVR and UTE)	9-11 12
▪ Motion during MR and/or PET data acquisition ▪ Motion between MR-based attenuation map and PET data acquisition	▪ MR-derived motion fields applied to PET reconstruction ▪ Acquisition of multi-phase MR-based AC maps during breathing and co-reconstruction of list-mode PET-data to matching AC phase	13-15

Table 1: Technical challenges and current correction methods for AC & MC in integrated PET/MR hybrid imaging.

CONCLUSION

Integrated whole-body PET/MR imaging has entered the clinical arena (1). On the physics and hardware development level, this opens up completely new options for medical imaging research (Table 1). Hardware component and tissue AC, MR-based motion correction for PET imaging, development of dedicated RF coils and hardware components designed towards PET-transparency, and standardization efforts are only few examples of this exciting hybrid imaging field. Beyond the scope of initial clinical PET/CT vs. PET/MR comparison studies, integrated PET/MR hybrid imaging is now under evaluation to define its diagnostic value in various clinical applications in oncology, neurology, cardiology, pediatric imaging, and therapy planning and monitoring. Already today neurologic diagnostic imaging and therapy monitoring in pediatric oncology emerge as potential key applications of integrated PET/MR (1). The use of various radiotracers, administration of MR contrast agent, and dedicated MR sequences for specific indications will unveil the full diagnostic potential of this new hybrid imaging modality.

REFERENCES

1. Quick HH. Integrated PET/MR. J Magn Reson Imag. 2013 Dec 12. Doi:10.1002/jmri.24523. [Epub].
2. Delso G, Fürst S, Jakoby B, et al. Performance measurements of the Siemens mMR integrated whole-body PET/MR scanner. J Nucl Med. 2011;52:1914–1922.
3. Delso G, Martinez-Möller A, Bundschuh RA, et al. Evaluation of the attenuation properties of MR equipment for its use in a whole-body PET/MR scanner. Phys Med Biol. 2010;55:4361-4374.
4. Tellmann L, Quick HH, Bockisch A, Herzog H, Beyer T. The effect of MR surface coils on PET quantification in whole-body PET/MR. Med Phys. 2011;38:2795-2805.
5. Paulus DH, Braun H, Aklan B, Quick HH. Simultaneous PET/MR imaging: MR-based attenuation correction of local radiofrequency surface coils Med. Phys. 2012;39:4306-4315.
6. Paulus DH; Tellmann L, Quick HH. Towards improved hardware component AC in PET/MR hybrid imaging. Phys Med Piol. 2013; 58:8021-8040.
7. Aklan B, Paulus DH, Wenkel E, et al. Toward simultaneous PET/MR breast imaging: systematic evaluation and integration of a radiofrequency breast coil. Med Phys. 2013;40:024301.
8. Martinez-Möller A, Souvatzoglou M, Delso G, et al. Tissue classification as a potential approach for AC in whole-body PET/MRI: evaluation with PET/CT data. J Nucl Med. 2009;50:520-526.
9. Samarin A, Burger C, Wollenweber SD, et al. PET/MR imaging of bone lesions - implications for PET quantification from imperfect attenuation correction. Eur J Nucl Med Mol Imaging. 2012;39:1154-1160.
10. Keereman V, Fierens Y, Broux T, De Deene Y, Lonneux M, Vandenberghe S. MRI-based attenuation correction for PET/MRI using ultrashort echo time sequences. J Nucl Med. 2010;51:812-818.
11. Johansson A, Karlsson M, Nyholm T. CT substitute derived from MRI sequences with ultrashort echo time. Med Phys. 2011;38:2708-2714.
12. Navalpakkam BK, Braun H, Kuwert T, Quick HH. Magnetic Resonance-Based Attenuation Correction for PET/MR Hybrid Imaging Using Continuous Valued Attenuation Maps. Invest Radiol. 2013;48:323-332.
13. Catana C, Benner T, van der Kouwe A, et al. MRI-assisted PET motion correction for neurologic studies in an integrated MR-PET scanner. J Nucl Med. 2011;52:154-161.
14. Tsoumpas C, Mackewn JE, Halsted P, et al. Simultaneous PET-MR acquisition and MR-derived motion fields for correction of non-rigid motion in PET. Ann Nucl Med. 2010;24:745-750.
15. Grimm R, Fürst S, Dregely I, et al. MR-PET Respiration compensation using self-gated motion modeling. In: Proceedings of the 21th Annual Meeting of ISMRM, Salt Lake City, 2013. (abstract 829).
16. Wiesmüller M, Quick HH, Lell M, et al. Comparison of lesion detection between PET from a simultaneously acquiring whole-body PET/MR hybrid scanner and PET from PET/CT. EJNMMI. 2013;40:12-21.
17. Drzezga A, Souvatzoglou M, Eiber M, et al. First Clinical Experience with Integrated Whole-Body PET/MR: Comparison to PET/CT in Patients with Oncologic Diagnoses. J Nucl Med. 2012;53:845-855.
18. Quick HH, von Gall C, Zeilinger M, et al. Integrated Whole-Body PET/MR Hybrid Imaging: Clinical Experience. Invest Radiol. 2013;48:280-289.
19. Schwenzer NF, Schraml C, Müller M, et al. Pulmonary lesion assessment: comparison of whole-body hybrid MR/PET and PET/CT imaging--pilot study. Radiology. 2012;264:551-558.
20. Bisdas S, Ritz R, Bender B, et al. Metabolic Mapping of Gliomas Using Hybrid MR-PET Imaging: Feasibility of the Method and Spatial Distribution of Metabolic Changes. Invest Radiol. 2013;48:295-301.
21. Stegger L, Martirosian P, Schwenzer N, et al. Simultaneous PET/MR imaging of the brain: feasibility of cerebral blood flow measurements with FAIR-TrueFISP arterial spin labeling MRI. Acta Radiol. 2012;53:1066-1072.
22. Barthel H, Gertz HJ, Dresel S, et al. Florbetaben Study Group. Cerebral amyloid-β PET with florbetaben (18F) in patients with Alzheimer's disease and healthy controls: a multicentre phase 2 diagnostic study. Lancet Neurol. 2011;10:424-435.
23. Hirsch FW, Sattler B, Sorge I, et al. PET/MR in children. Initial clinical experience in paediatric oncology using an integrated PET/MR scanner. Pediatr Radiol. 2013;43:860-875.